Oxford, **1996**, pp. 43–83; b) D. L. Caulder, K. N. Raymond, *Acc. Chem. Res.* **1999**, *32*, 975–982; c) D. L. Caulder, K. N. Raymond, *J. Chem. Soc. Dalton Trans.* **1999**, *8*, 1185–1200; d) M. Fujita, *Chem. Soc. Rev.* **1998**, *6*, 417–425; e) S. Leininger, B. Olenyuk, P. J. Stang, *Chem. Rev.* **2000**, *100*, 853–908; f) E. Uller, B. Demleitner, I. Bernt, R. W. Saalfrank, *Struct. Bonding* **2000**, *96*, 149–175.

[3] a) D. M. L. Goodgame, S. Menzer, A. M. Smith, D. J. Williams, *J. Chem. Soc. Dalton Trans.* **1997**, 3213–3218; b) O. M. Yaghi, C. E. Davis, G. Li, H. Li, *J. Am. Chem. Soc.* **1997**, *119*, 2861–2868; c) M. J. Zaworotko, *Chem. Soc. Rev.* **1994**, *23*, 283–288; d) K. A. Hirsch, S. C. Wilson, J. S. Moore, *Chem. Eur. J.* **1997**, *3*, 765–771.

[4] a) I. Huc, J.-M. Lehn, *Proc. Natl. Acad. Sci. USA* **1997**, *94*, 2106–2110; b) D. P. Funeriu, J.-M. Lehn, G. Baum, D. Fenske, *Chem. Eur. J.* **1997**, *3*, 99–104; c) P. N. W. Baxter, J.-M. Lehn, K. Rissanen, *Chem. Commun.* **1997**, 1323–1324.

[5] B. Hasenknopf, J.-M. Lehn, N. Boumediene, A. Dupont-Gervais, A. van Dorsselaer, B. Kneisel, D. Fenske, *J. Am. Chem. Soc.* **1997**, *119*, 10956–10962.

[6] K. Kasai, M. Aoyagi, M. Fujita, *J. Am. Chem. Soc.* **2000**, *122*, 2140–2141.

[7] D. Braga, F. Grepioni, G. R. Desiraju, *Chem. Rev.* **1998**, *98*, 1375–1405.

[8] Crystal structure analysis of **1** at 200(1) K: $C_{46}H_{32}N_4O_8F_{24}Mn_2$, $M_r = 1334.64$, yellow prism, $0.33 \times 0.25 \times 0.08$ mm, monoclinic space group C_2, $a = 20.5454(7)$, $b = 11.7067(4)$, $c = 12.7161(5)$ Å, $\alpha = 90$, $\beta = 114.4019(18)$, $\gamma = 90°$, $V = 2785.25(15)$ Å^3, $Z = 2$, $\rho_{calcd} = 1.591$ g cm^{-3}, $Mo_{K\alpha}$ radiation $\lambda = 0.71073$ Å, $\mu = 0.586$ mm^{-1}. Data were collected on a Nonius KappaCCD diffractometer in the range $3.90 < 2\theta < 30.07°$. A total of 6949 measured reflections, 6949 unique, 4951 with $F_0^2 > 4\sigma(F_0^2)$ were used to refine 536 parameters to $R1(wR2) = 0.0501(0.1037)$, GOF = 1.011, F^2 refinement in SHELXL97. A multiscan absorption correction gave min. and max. transmission factors of 0.9546 and 0.8301. The residual peaks in the final difference map ranged from -0.229 to $+0.707$ e Å^3. All four CF_3 groups are disordered in two different orientations with a nearly 50:50 occupancy. The 1,3-bpyp ligand was found also to be disordered in two slightly different orientations with a major orientation of 70%.[14]

[9] O. J. Gelling, F. van Bolhuis, B. L. Feringa, *J. Chem. Soc. Chem. Commun.* **1991**, 917–919.

[10] T. Ezuhara, K. Endo, Y. Aoyama, *J. Am. Chem. Soc.* **1999**, *121*, 3279–3283.

[11] Several crystals of different product batches showed, by circular dichroism (CD) spectroscopy, the apparently random distribution of *P*- and *M*-helices.

[12] Crystal structure analysis of **2** at 200(1) K: $C_{52}H_{38}N_4O_8F_{24}Mn_2$, $M_r = 1412.74$, yellow prism, $0.23 \times 0.20 \times 0.20$ mm, triclinic space group $P\bar{1}$, $a = 10.2719(7)$, $b = 12.9946(9)$, $c = 13.0612(7)$ Å, $\alpha = 61.494(4)$, $\beta = 83.550(4)$, $\gamma = 81.017(3)°$, $V = 1511.82(17)$ Å^3, $Z = 1$, $\rho_{calcd} = 1.552$ g cm^{-3}, $Mo_{K\alpha}$ radiation $\lambda = 0.71073$ Å, $\mu = 0.545$ mm^{-1}. Data were collected on a Nonius KappaCCD diffractometer in the range $2.50 < 2\theta < 26.02°$. A total of 8635 measured reflections, 5881 unique, 4488 with $F_0^2 > 4\sigma(F_0^2)$ were used to refine 407 parameters to $R1(wR2) = 0.0565(0.1342)$, GOF = 1.039, F^2 refinement in SHELXL97. A multiscan absorption correction gave min. and max. transmission factors of 0.8989 and 0.8849. The highest peak in the final difference map ranged from -0.436 to $+0.604$ e Å^3.[14]

[13] Crystal structure analysis of **3** at 200(1) K: $C_{60}H_{46}N_4O_8F_{24}Mn_2$, $M_r = 1516.89$, yellow prism, $0.25 \times 0.23 \times 0.20$ mm, monoclinic space group $P2_1/n$, $a = 10.2946(1)$, $b = 28.1849(5)$, $c = 22.6755(5)$ Å, $\alpha = 90$, $\beta = 98.3108(10)$, $\gamma = 90°$, $V = 6510.25(19)$ Å^3, $Z = 4$, $\rho_{calcd} = 1.548$ g cm^{-3}, $Mo_{K\alpha}$ radiation $\lambda = 0.71073$ Å, $\mu = 0.512$ mm^{-1}. Data were collected on a Nonius KappaCCD diffractometer in the range $2.20 < 2\theta < 26.05°$. A total of 22624 measured reflections, 12755 unique, 7936 with $F_0^2 > 4\sigma(F_0^2)$ were used to refine 1003 parameters to $R1(wR2) = 0.0576(0.1186)$, GOF = 1.022, F^2 refinement in SHELXL97. A multiscan absorption correction gave min. and max. transmission factors of 0.9045 and 0.8827. The residual peaks in the final difference map ranged from -0.347 to $+0.318$ e Å^3. Four CF_3 groups were disordered in two different orientations with partial occupancy ranging from 0.75 to 0.92. The 1,2-dphe molecule was also disordered in two slightly different orientations with a major orientation of nearly 60%.[14]

[14] Crystallographic data (excluding structure factors) for the structures reported in this paper have been deposited with the Cambridge Crystallographic Data Centre as supplementary publication no. CCDC-153290, CCDC-153291, and CCDC-153292. Copies of the data can be obtained free of charge on application to CCDC, 12 Union Road, Cambridge CB2 1EZ, UK (fax: (+44) 1223-336-033; e-mail: deposit@ccdc.cam.ac.uk).

Ultrafast Electron Diffraction of Transient $[Fe(CO)_4]$: Determination of Molecular Structure and Reaction Pathway**

Hyotcherl Ihee, Jianming Cao, and Ahmed H. Zewail*

Transition metal carbonyl complexes[1, 2] respond to ultraviolet light by the loss of one or more CO ligands and subsequent formation of coordinatively unsaturated carbonyl complexes, which are known to catalyze a variety of reactions.[3–5] The photochemistry governing the formation of these coordinatively unsaturated species has been an active area of research both experimentally[6–13] and theoretically,[14–19] often focusing on the reaction pathways and molecular structures of these transient species. Among transition metal carbonyl complexes, $[Fe(CO)_5]$ is one of the most extensively studied molecular systems. $[Fe(CO)_5]$ absorbs strongly in the ultraviolet starting at about 350 nm (3.5 eV).[18, 20–22] The spectrum is rather featureless, and is dominated by metal-to-ligand charge transfer transitions[18] at high energies. Having five carbonyl ligands, an $[Fe(CO)_5]$ molecule can dissociate into five different products ($[Fe(CO)_x]$, $x = 4, 3, 2, 1, 0$) depending on the excitation wavelength.

In these reactions, $[Fe(CO)_4]$ is the primary intermediate and serves as a "doorway" molecule for various subsequent reactions,[23, 24] such as decomposition, recombination with the carbonyl ligand, and coordination with solvent molecules. Elucidating the nature of $[Fe(CO)_4]$, including its electronic states and the corresponding molecular geometry, is important for understanding the role of intermediates in the photolysis of transition metal carbonyl complexes.

Herein we report the direct determination of the molecular structure (Figure 1) of transient $[Fe(CO)_4]$ using diffraction with ultrashort pulses of electrons. In this way, we are able to identify the primary reaction pathway and provide details of

[*] Prof. A. H. Zewail, H. Ihee, Dr. J. Cao[+]
Laboratory for Molecular Sciences
Arthur Amos Noyes Laboratory of Chemical Physics
California Institute of Technology
Pasadena, CA 91125 (USA)
Fax: (+1) 626-796-8315
E-mail: zewail@caltech.edu

[+] Present address: National High Magnetic Field Laboratory
Florida State University
1800 East Paul Dirac Drive
Tallahassee, FL 32310 (USA)

[**] This work was supported by grants from the National Science Foundation, Air Force Office of Scientific Research, and the Office of Naval Research.

  0044-8249/01/11308-1580 $ 17.50+.50/0

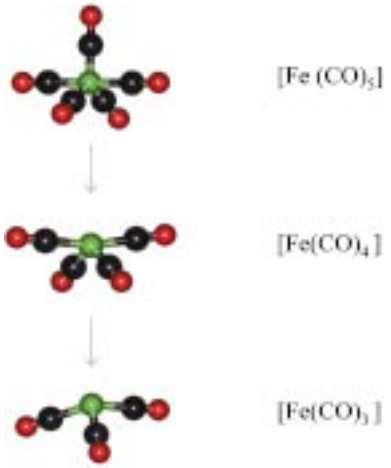

Figure 1. Structural changes accompanying the elimination of CO ligands from $[Fe(CO)_5]$.

bond lengths and angles of the intermediate structure. Because of the picosecond time resolution invoked in these ultrafast electron diffraction (UED) experiments, it is possible to "freeze" the intermediate and determine its structure and pathway. For $[Fe(CO)_4]$, we provide direct evidence that the molecular structure involved is that of the singlet, not triplet, pathway contrary to many suggestions in past studies.

The potential energy levels of the $[Fe(CO)_x]$ species relevant to the photolysis of $[Fe(CO)_5]$ are shown in Figure 2. The ground state of $[Fe(CO)_5]$ is a singlet ($^1A_1'$; D_{3h}) and can be pumped into excited singlet states by absorbing ultraviolet photons. Two possible reaction pathways, the singlet and the triplet, following UV excitation have been postulated.[8, 9, 13, 14, 16, 25] In the singlet pathway,[8, 13, 25] the $^1E'$ state molecules of $[Fe(CO)_5]$ dissociate into the singlet excited state ($^1A_1$) of $[Fe(CO)_4]$, while for the triplet pathway,[8, 9, 16] intersystem crossing to the $^3E'$ state of $[Fe(CO)_5]$ is required prior to dissociation to the triplet ground state ($^3B_2$) of $[Fe(CO)_4]$. For photolysis in solid matrices at low temperature, the produced $[Fe(CO)_4]$ was characterized[26] to have a structure with C_{2v} symmetry and to be in the triplet electronic ground state. This observation is consistent with other experimental results in which secondary fragments ($[Fe(CO)_3]$, $[Fe(CO)_2]$, and $[Fe(CO)]$) in their triplet electronic ground states were observed as major products, indicating that the ground state ($^3B_2$) of $[Fe(CO)_4]$ played a determining role.[9, 10, 27]

However, it was still unclear whether $[Fe(CO)_4]$ is formed directly into the triplet state or through relaxation via singlet states (Figure 2), and how the reaction proceeds to generate the subsequent secondary fragments. Early studies on the nanosecond time scale have suggested that the fragmentation follows the triplet pathway.[9, 10] A more recent study has suggested that the $^1A_1$ state is initially formed via a very short-lived higher state of $[Fe(CO)_4]$, favoring the singlet pathway.[13] The discrepancy may originate from the difficulty associated with directly monitoring the identity of transient intermediate structure during the course of the reaction. In this respect, UED[28–32] is a powerful method for studying the

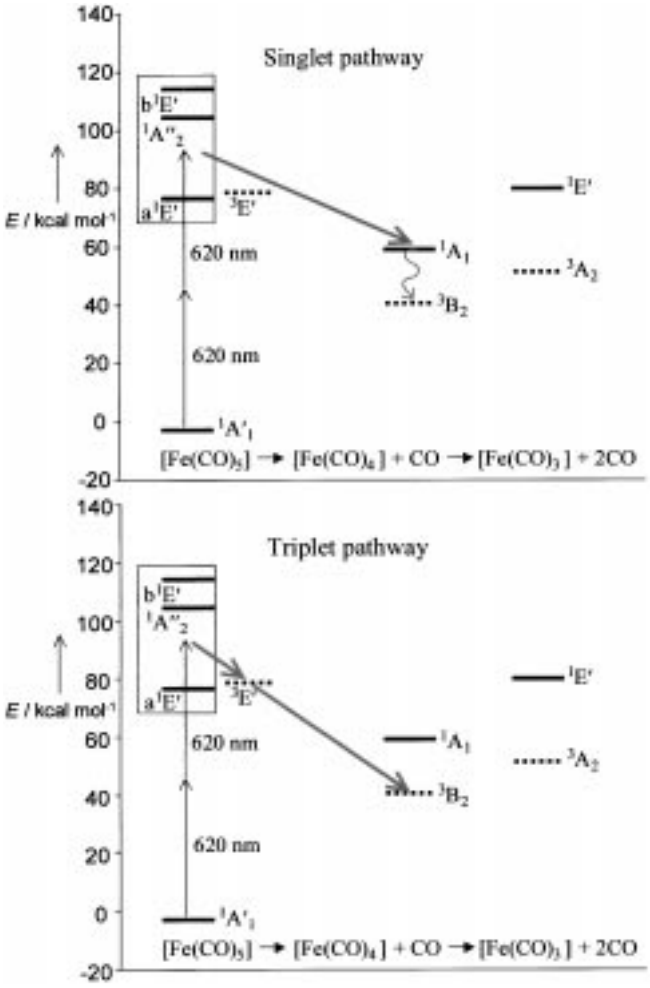

Figure 2. Scheme of the potential energy levels and pathways of the UV dissociation of $[Fe(CO)_5]$. The following energies (in kcal mol^{-1}) relative to the ground state ($^1A_1'$) of $[Fe(CO)_5]$ are from the literature.[10, 14, 15, 17, 18] $[Fe(CO)_5]$: $^3E'$ 78.1, a^1E' 77.2, $^1A_2''$ 105.8, b^1E' 114.4; $[Fe(CO)_4]$: $^3B_2$ 41.5, $^1A_1$ 59.0, $[Fe(CO)_3]$: $^3A_2$ 53.0, $^1E'$ 80.7. The two pathways, singlet and triplet, are indicated in the two panels.

molecular structure of transient $[Fe(CO)_4]$. As with conventional ultrafast spectroscopies,[33, 34] UED utilizes a femtosecond (fs) laser pulse to initiate a desired chemical reaction; however in UED, the subsequent laser pulses normally used to probe the progress of the reaction are replaced with ultrashort pulses of electrons. Diffraction patterns are then recorded to provide the internuclear distances of the molecular species involved.

The UED experiments on $[Fe(CO)_5]$ were performed by using the second-generation apparatus[28] developed in this laboratory. The time zero, when the excitation laser pulse and the probing electron pulse temporally overlap in the molecular beam, was determined by an ion-induced lensing experiment[28] with ± 2 ps accuracy. To initiate the reaction, a fs laser pulse was focused into the gas sample beneath the needle of the free-jet expansion. The snapshots of diffraction images at a certain delay time t (-180 and $+200$ ps) were recorded and converted to the diffraction intensity data $I_{tot}(t; s)$, where $s = (4\pi/\lambda)\sin(\theta/2)$, λ is the de Broglie wavelength of the electrons, and θ is the scattering angle.

  0044-8249/01/11308-1581 $ 17.50+.50/0

In our experiments, the time zero was determined with 2 ps accuracy and the overall temporal resolution was less than 20 ps. Thus the diffraction data obtained when probe electron pulses arrived 180 ps ahead of excitation laser pulses (I_{tot} (-180 ps; s)) provided a reference signal originated only from the parent molecules [$Fe(CO)_5$], as these parent molecules were not excited by the initiating laser. In contrast, the data at $+200$ ps, I_{tot} ($+200$ ps; s), comprises the contributions from both the remaining parent molecules, [$Fe(CO)_5$], and newly formed photoproducts, [$Fe(CO)_x$]. Thus, the difference between them [Eq. (1)][29–32] selects the reaction change induced by the fs laser pulse.

$$\Delta I_{tot}(+200\ \text{ps}; -180\ \text{ps}; s) = I_{tot}(+200\ \text{ps}; s) - I_{tot}(-180\ \text{ps}; s), \quad (1)$$

In the diffraction difference signal, ΔI_{tot}, the contributions from unreacted molecules and the background signal, which do not change in the course of the chemical reaction, are eliminated, thus highlighting the signal from the change in molecular structure under consideration.[35] For data analysis, the difference modified molecular scattering intensity, $\Delta sM(t; t_{ref}; s)$, was obtained following the conventional definition given in Equation (2),[36] where I_{atom} is the atomic scattering intensity ($t = +200$ ps and $t_{ref} = -180$ ps in the present case).

$$\Delta sM(t; t_{ref}; s) = s\Delta I(t; t_{ref}; s)/(I_{atom}), \quad (2)$$

The corresponding difference radial distribution curves, $\Delta f(r)$, which directly give the change in internuclear distances (r) of the reaction, were then calculated from the $\Delta sM(s)$ curves according to the standard gas-phase electron diffraction equation (3),[36] where the constant $k = 0.02$ Å^2, is a damping coefficient included to account for the limited s range.

$$\Delta f(r) = \int_0^{s_{max}} \Delta sM(s)\sin(sr)\exp(-ks^2)ds \quad (3)$$

With two-photon excitation at the wavelength of 620 nm, only [$Fe(CO)_4$] (both $^1A_1$ and $^3B_2$ states) and [$Fe(CO)_3$] (the $^3A_2$ state only)[37] are energetically possible. A fit with these three possible products was performed by floating the fraction (relative to 100% parent fraction before the photolysis) of each species, and by using the structural parameters obtained from ab initio calculations.[19] The fraction of the singlet [$Fe(CO)_4$] was 14 ± 1%, while the total fraction of the triplet [$Fe(CO)_4$] and triplet [$Fe(CO)_3$] was less than 1%, indicating that the singlet [$Fe(CO)_4$] is the primary product and the formation of other species is negligible. To trace other possible secondary photofragments, a fit including triplet [$Fe(CO)_2$], triplet [Fe(CO)], and Fe was also performed by floating the fraction of each species, while keeping their structural parameters fixed at the values obtained from ab initio calculations.[19] The resulting total fraction of [$Fe(CO)_2$], [Fe(CO)], and Fe was less than 1%, confirming that these secondary products are negligible.

Figure 3 shows the comparison between the UED data fits with [$Fe(CO)_4$] for the two different reaction pathways. The [$Fe(CO)_4$] structure in the $^1A_1$ state is very similar to that of [$Fe(CO)_5$] with one equatorial carbonyl group removed, while

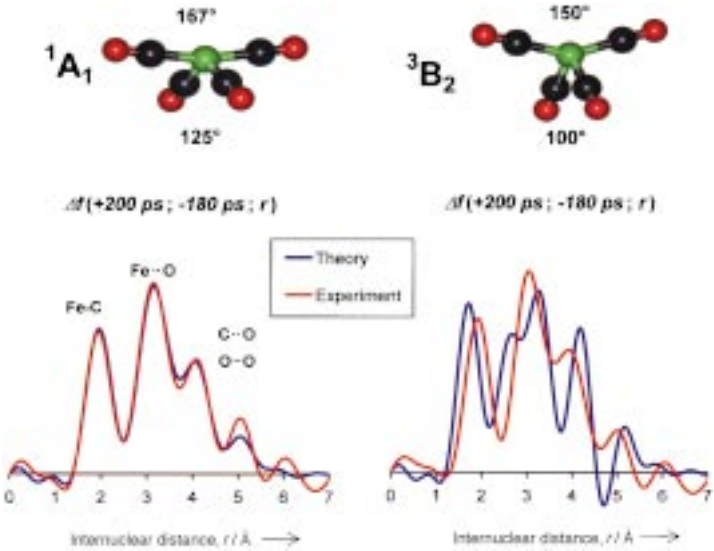

Figure 3. Ultrafast electron diffraction of the intermediate [$Fe(CO)_4$] species. Top: The structures of two possible electronic states ($^1A_1$ and $^3B_2$) for [$Fe(CO)_4$]. The values for the angles are from ab initio calculations.[19] Bottom: Comparison of experimental $-\Delta f(+200\ \text{ps}; -180\ \text{ps}; r)$ curves (red) with corresponding theoretical calculations (blue) obtained from ab initio structures of the $^1A_1$ state (left) and the $^3B_2$ state (right).

the structure of [$Fe(CO)_4$] in the $^3B_2$ state is significantly distorted.[19] The C-Fe-C angles of the $^3B_2$ state are smaller and the Fe–C distances are longer than those of [$Fe(CO)_5$]. As shown in Figure 3, the fit for the $^3B_2$ state is clearly inferior to that of the $^1A_1$ state, which gives a very good agreement between the experiment and theory. Therefore, [$Fe(CO)_4$] is formed following the singlet pathway of the reaction in its singlet excited state, $^1A_1$, rather than the ground state, $^3B_2$, at the exciation used.[38] The $^1A_1$ state [$Fe(CO)_4$] may eventually convert into the $^3B_2$ state through intersystem crossing (thereby providing a more efficient route for the formation of the $^3A_2$ state [$Fe(CO)_3$]), but intersystem crossing needs more than 200 ns,[11, 25] which is beyond our investigated time range of up to 200 ps.

A closer examination of the $\Delta f(+200\ \text{ps}; -180\ \text{ps}; r)$ curve (Figure 3) reveals rich details of the structural changes due to the depletion of [$Fe(CO)_5$] and formation of [$Fe(CO)_4$]. The two main peaks centered at about 2 Å and about 3 Å, respectively, indicate the depletion of the Fe – C and Fe···O internuclear contributions due to the liberation of CO. The shoulders beyond 3.5 Å are due to the reduction of other internuclear contributions, C···O and O···O, in the liberation process. The small peak for the C–O bond at about 1.12 Å is negative because the liberated CO ligand has a shorter bond length than that of the bound ligand ($\sim$1.15 Å), but the negative amplitude of the peak is small because the change (from 1.15 Å to 1.12 Å) is minute, causing the positive and negative contributions to nearly cancel out.

The structure of [$Fe(CO)_4$] obtained from our UED experiment was futher refined by limiting the fit to a single product and floating all the independent structural parameters. The results are shown in Figure 4 and give the following structural parameters: r(Fe–C1) = 1.81 ± 0.03 Å, r(C1–O1) = 1.14 ± 0.05 Å, r(Fe–C2) = 1.77 ± 0.03 Å; r(C2–O2) = $1.15 \pm$

  0044-8249/01/11308-1582 $ 17.50+.50/0

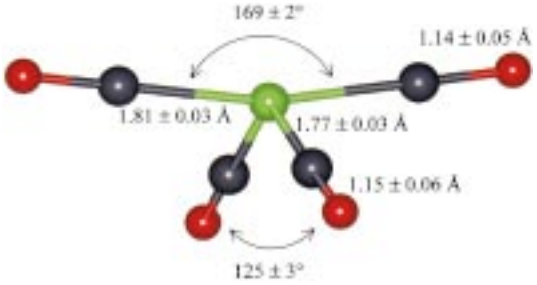

Figure 4. The refined molecular structure of $[Fe(CO)_4]$ in the $^1A_1$ state, determined by ultrafast electron diffraction (see text).

0.06 Å, $\sphericalangle$C1-Fe-C1 $= 169 \pm 2°$, $\sphericalangle$C2-Fe-C2 $= 125 \pm 3°$. The error bars represent one standard deviation and do not account for systematic errors. The structure determined here is in good agreement with that determined by ab initio calculation[19] for the $^1A_1$ state. Much earlier, Poliakoff and Turner in their studies of $[Fe(CO)_4]$ found a species other than the triplet ground state and tentatively assigned the species to be in the singlet state stabilized by a CH_4 matrix at low temperatures. Their careful analysis of IR intensities led them to obtain $173.5 \pm 1°$ and $125 \pm 2.5°$ for C-Fe-C angles,[26] which are remarkably close to our experimental UED values obtained for the isolated species.

In summary, the UED technique was used to study the elimination of CO ligands from $[Fe(CO)_5]$. The molecular structure of the transient species was identified by using the temporal diffraction-difference approach of UED. Our results clearly showed that the major product, up to 200 ps, is the transient $[Fe(CO)_4]$ formed in the $^1A_1$ state, rather than the ground $^3B_2$ state. The structure obtained from the diffraction data was further refined to give the bond lengths and angles of the transient $[Fe(CO)_4]$ with a resolution of about 0.05 Å. This combined temporal and structural resolution should be of significant value in identifying transition configurations and pathways of other reactions.

Experimental Section

The second-generation UED apparatus[28] is composed of a femtosecond laser, a picosecond electron gun, a free-jet expansion sample source, and a two-dimensional single-electron detection system. Femtosecond laser pulses from a colliding-pulse mode-locked ring dye laser were amplified in a four-stage pulsed dye amplifier pumped by a Nd:YAG laser. The amplified pulses (620 nm, 3 mJ pulse^{-1}, 30 Hz, ~300 fs pulse width) were then split into pump and probe laser pulses; 95% of each laser pulse (pump) was directed and focused into the gas sample beneath the needle of the free-jet expansion source in the scattering chamber. The remaining 5% (probe) was first frequency-doubled with a potassium dihydrogen phosphate crystal, and then focused onto a back-illuminated photocathode in the electron gun to generate the ps electron pulses.

The ultrashort electron pulses were accelerated to 18.8 keV (de Broglie wavelength is 0.088 Å) and focused into the scattering volume. The two-dimensional diffraction images were recorded at chosen delay times by a charge-coupled device camera at the end of a phosphor scintillator/fiber optic/image intensifier chain in the detection chamber. The electron pulse, laser pulse, and molecular beam were arranged in a cross-beam geometry, and the alignment of the three beams was controlled to within 10 μm. Time delays between the fs pump laser pulse and the ps electron pulse were controlled by a computer-driven translational stage. The diffraction images were taken with ultrashort electron pulses (~2×10^4 electrons per pulse, with temporal width of 15 ps), and the total temporal resolution is less than 20 ps. The beam waist of both the electron beam and laser beam was adjusted to be about 300 μm, and the camera length was measured to be 102.9 mm. This second-generation apparatus is now replaced with a third-generation machine which provides orders of magnitude improvement in time resolution and sensitivity.[32]

$[Fe(CO)_5]$ was purchased from Aldrich (98% purity). The sample was first purified through vacuum distillation and then transferred into a sample cell in situ. Following connection to the diffraction chamber, the sample was degassed by three cycles of freeze-pump-thaw. To provide enough molecular gas density in the scattering volume, the sample cell, gas line, and nozzle were heated to 47, 64, and 72 °C, respectively. The gas pressure in the scattering chamber during the experiment was about 4.6×10^{-4} Torr, and the pressure at the scattering volume was estimated to be about a few Torr.

Received: December 29, 2000 [Z16350]

[1] G. L. Geoffroy, M. S. Wrighton, *Organometallic Photochemistry*, Academic Press, New York, **1979**, and references therein.
[2] G. A. Ozin, A. J. L. Hanlan, *Inorg. Chem.* **1979**, *18*, 2091.
[3] M. S. Wrighton, D. S. Ginley, M. A. Schroeder, D. L. Morse, *Pure Appl. Chem.* **1975**, *41*, 671.
[4] I. Wender, P. Pino, *Organic Synthesis via Metal Carbonyls*, Wiley, New York, **1977**.
[5] M. A. Schroeder, M. S. Wrighton, *J. Am. Chem. Soc.* **1976**, *98*, 551.
[6] J. T. Yardley, B. Gitlin, G. Nathanson, A. M. Rosan, *J. Chem. Phys.* **1981**, *74*, 370.
[7] R. L. Whetten, K.-J. Fu, E. R. Grant, *J. Chem. Phys.* **1983**, *79*, 4899.
[8] T. A. Seder, A. J. Ouderkirk, E. Weitz, *J. Chem. Phys.* **1986**, *85*, 1977.
[9] I. M. Waller, J. W. Hepburn, *J. Chem. Phys.* **1988**, *88*, 6658.
[10] B. K. Venkataraman, G. Bandukwalla, Z. Zhang, M. Vernon, *J. Chem. Phys.* **1989**, *90*, 5510.
[11] R. J. Ryther, E. Weitz, *J. Phys. Chem.* **1991**, *95*, 9841.
[12] L. Bañares, T. Baumert, M. Bergt, B. Kiefer, G. Gerber, *J. Chem. Phys.* **1998**, *108*, 5799.
[13] S. A. Trushin, W. Fuss, K. L. Kompa, W. E. Schmid, *J. Phys. Chem. A* **2000**, *104*, 1997.
[14] C. Daniel, M. Benard, A. Dedieu, R. Wiest, A. Veillard, *J. Phys. Chem.* **1984**, *88*, 4805.
[15] D. Guenzburger, E. M. B. Saitovitch, M. A. De Paoli, H. Manela, *J. Chem. Phys.* **1984**, *80*, 735.
[16] A. Veillard, A. Strich, C. Daniel, P. E. M. Siegbahn, *Chem. Phys. Lett.* **1987**, *141*, 329.
[17] L. A. Barnes, M. Rosi, C. W. J. Bauschlicher, *J. Chem. Phys.* **1991**, *94*, 2031.
[18] O. Rubner, V. Engel, M. R. Hachey, C. Daniel, *Chem. Phys. Lett.* **1999**, *302*, 489.
[19] O. González-Blanco, V. Branchadell, *J. Chem. Phys.* **1999**, *110*, 778.
[20] M. Dartiguenave, Y. Dartiguenave, H. B. Gray, *Bull. Soc. Chim. Fr.* **1969**, *12*, 4223.
[21] G. Nathanson, B. Gitlin, A. M. Rosan, J. T. Yardley, *J. Chem. Phys.* **1981**, *74*, 361.
[22] M. Kotzian, N. Rosch, H. Schroder, M. C. Zerner, *J. Am. Chem. Soc.* **1989**, *111*, 7687.
[23] M. Wrighton, *Chem. Rev.* **1974**, *74*, 401.
[24] M. Poliakoff, E. Weitz, *Acc. Chem. Res.* **1987**, *20*, 408.
[25] R. J. Ryther, E. Weitz, *J. Phys. Chem.* **1992**, *96*, 2561.
[26] M. Poliakoff, J. J. Turner, *J. Chem. Soc. Dalton Trans.* **1974**, 2276.
[27] A. J. Ouderkirk, P. Wermer, N. L. Schultz, E. Weitz, *J. Am. Chem. Soc.* **1983**, *105*, 3354.
[28] J. C. Williamson, J. Cao, H. Ihee, H. Frey, A. H. Zewail, *Nature* **1997**, *386*, 159.
[29] H. Ihee, J. Cao, A. H. Zewail, *Chem. Phys. Lett.* **1997**, *281*, 10.
[30] J. Cao, H. Ihee, A. H. Zewail, *Chem. Phys. Lett.* **1998**, *290*, 1.
[31] J. Cao, H. Ihee, A. H. Zewail, *Proc. Natl. Acad. Sci. USA* **1999**, *96*, 338.
[32] H. Ihee, V. A. Lobastov, U. Gomez, B. M. Goodson, R. Srinivasan, C.-Y. Ruan, A. H. Zewail, *Science* **2001**, *291*, 458.
[33] A. H. Zewail, *Femtochemistry: Ultrafast Dynamics of the Chemical Bond*, World Scientific, Singapore, **1994**.
[34] J. Manz, L. Wöste, *Femtosecond Chemistry*, VCH, New York, **1995**.

  0044-8249/01/11308-1583 $ 17.50+.50/0

[35] A smooth residual background with extremely small amplitude, a likely result of the interaction of probe electrons with positive ions in the gas sample generated by the intense laser pulses,[29] was observed in our experimental ΔI_{tot}. The background was removed by fitting a smooth curve through the zero-crossing points of the theoretical ΔI_{tot}.[29–32] The experimental ΔI_{tot} curve was smoothed by Fourier filtering[32] (9 Å low-pass) and pixel regions showing systematic abnormalities were removed.[32]

[36] I. Hargittai, M. Hargittai, *Stereochemical Applications Of Gas-Phase Electron Diffraction*, VCH, New York, **1988**.

[37] The singlet $[Fe(CO)_3]$ may, in principle, be generated through subsequent loss of a CO ligand from the singlet $[Fe(CO)_4]$. However, consideration of the energetics eliminates this possibility. The total energy available following the dissociation of $[Fe(CO)_5]$ into $[Fe(CO)_4]$ and CO upon two-photon excitation at 620 nm (92 kcal mol^{-1}) is 33 kcal mol^{-1}, and at most about 65% (21 kcal mol^{-1}) of this remaining energy is retained as the internal excitation of $[Fe(CO)_4]$.[6, 9, 11] Since the energy gap between the singlet $[Fe(CO)_4]$ and the singlet $[Fe(CO)_3]$ is at least 22 kcal mol^{-1}, the available energy is not enough to liberate another CO ligand.

[38] In our previous attempt[29] to isolate the $[Fe(CO)_4]$ species, 310 nm fs laser pulses were used to photolyze $[Fe(CO)_5]$. Although one photon of 310 nm just falls short of the threshold for generating $[Fe(CO)_2]$, [Fe(CO)] and Fe, it was found that in fact two-photon absorption dominated. Consequently, the major products obtained were actually $[Fe(CO)_2]$, [Fe(CO)], and Fe rather than $[Fe(CO)_4]$ or $[Fe(CO)_3]$. In the present experiment, 620 nm photon excitation was used instead of 310 nm and the main absorption is two-photon. This excitation provides enough energy to break at most two Fe–C bonds, leaving $[Fe(CO)_4]$ and $[Fe(CO)_3]$ as major products.

Dual-Signaling Fluorescent Chemosensors Based on Conformational Restriction and Induced Charge Transfer**

Jesse V. Mello and Nathaniel S. Finney*

Fluorescent chemosensors provide a powerful optical method for spying on molecular recognition events. As a result, they have found practical application in cellular imaging, environmental monitoring, and biological assays.[1] Chemosensors that allow the measurement of two different emissions bands have the important feature that they permit signal ratioing, which can increase the dynamic range and provide built-in correction for environmental effects.[2] In addition, dual-channel fluorophores allow a change in perceived color as well as simple brightening, facilitating rapid visual assays.

A common feature of dual-channel fluorescent chemosensors is that substrate binding leads to enhancement of one emission channel at the expense of the other. We describe herein an exception to this generalization, in which the combination of two signaling mechanisms—conformational restriction and induction of charge transfer—allows metal binding to turn two fluorescence emission bands on independently.[3]

Biarylpyridines **1**–**4** (Scheme 1) were chosen for the present study because of their synthetic accessibility and modest fluorescence emission from the locally excited (LE) state.[4]

The unanticipated emission from an induced charge transfer (CT) state further extends the versatility of these fluorophores.[5] The emission of **1** (1×10^{-5} M in CH_3CN) is illustrative: the neutral fluorophore exhibits strong LE emission at about 345 nm; on protonation of the pyridine nitrogen atom with trifluoroacetic acid, the LE emission is completely replaced by readily visible CT emission at about 450 nm (Figure 1).

Appending **1** with polyether metal binding domains leads to dual-channel fluorescent chemosensors that are remarkably responsive and selective given their structural simplicity. The titration of **2** (1×10^{-5} M in CH_3CN) with alkali metal and alkaline earth cations is representative (Figure 2). The addition of excess Li^+ leads to strong (5.5-fold at λ_{max}) enhancement of the emission from the LE state, and concomitant increase in quantum yield as a result of binding-induced conformational restriction.[6] In contrast, the addition of Mg^{2+} leads to a slight diminution of LE emission,

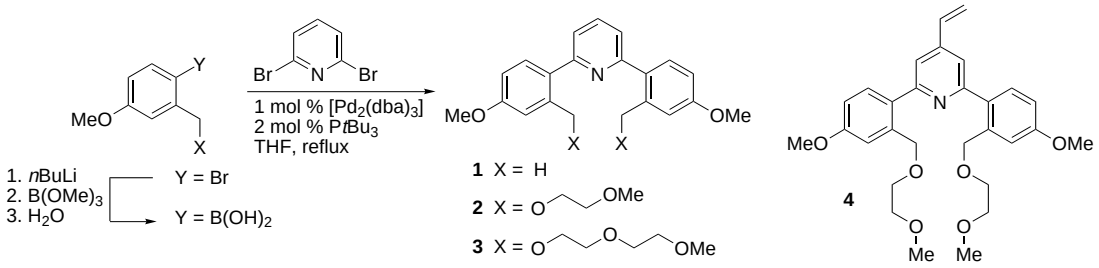

Scheme 1. Synthesis of biarylpyridines **1**–**4**. Compound **4** was synthesized analogously to **2** by using the 4-vinyl-substituted pyridine derivative. dba = *trans*,*trans*-dibenzylideneacetone.

[*] Prof. N. S. Finney, J. V. Mello
Department of Chemistry and Biochemistry
University of California, San Diego
La Jolla, CA 92093-0358 (USA)
Fax: (+1) 858-822-0386
E-mail: nfinney@chem.ucsd.edu

[**] The authors gratefully acknowledge the National Science Foundation for support of this research (CHE-9876333) and the Departmental NMR facilities (CHE-9709183), and the UC Toxic Substances Research and Teaching Program for support of this research.

but an enhancement of CT emission. Notably, the addition of Ca^{2+} leads to simultaneous enhancement of *both* emission bands (Figure 2). The K_a values for the association of **2** with Li^+, Mg^{2+}, and Ca^{2+} are 6.7×10^3 M^{-1}, 8.3×10^2 M^{-1}, and 6.7×10^2 M^{-1} respectively.[7, 8]

The seemingly minor structural change from **2** to **3** leads to a significantly altered metal-binding profile. While **3** still responds to Li^+, it does so only weakly compared to **2** (I/I_0 at

  0044-8249/01/11308-1584 $ 17.50+.50/0